https://doi.org/10.15407/ujpe70.6.391

A. JUMABAEV,[1] B. KHUDAYKULOV,[1] S.-J. KOYAMBO-KONZAPA,[2]
U. HOLIKULOV,[1] H. HUSHVAKTOV,[1] A. ABSANOV,[1] I. DOROSHENKO [1,3]

[1] Department of Optics and Spectroscopy, Samarkand State University
(University Blvd., Samarkand, 140104, Uzbekistan; e-mail: bekzodxudaykulov30@gmail.com)
[2] Laboratoire Matière, Energie et Rayonnement (LAMER), Université de Bangui
(P.O. Box 1450 Bangui, République Centrafricaine)
[3] Taras Shevchenko National University of Kyiv
(64/13, Volodymyrska Str., Kyiv 01601, Ukraine; e-mail: dori11@ukr.net)

EXPLORING NONCOVALENT INTERACTIONS OF THIOPHENE-2-CARBOXYLIC ACID IN ETHANOL VIA VIBRATIONAL SPECTROSCOPY AND DFT CALCULATIONS

The spectral bands of pure 2-thiophene carboxylic acid (TCA) and its solution in ethanol (EtOH) are investigated over a wide range using vibrational spectroscopy (Raman and FTIR). In the TCA solution with EtOH, the maxima of the C=O, O–H, C–H stretching, and C–H breathing vibration bands show either a redshift or a blueshift. This indicates that H-bonding, van der Waals interactions, and hyper-conjugation interactions are likely in solutions. MEPS, HOMO and LUMO, AIM, NCI, RDG, ELF, and LOL analyses are performed using a quantum chemical computational approach based on density functional theory (DFT). The MEPS map was used to visually show the charge distribution in the complexes and determine charge-dependent characteristics. Frontier molecular orbitals (FMO) have been utilized to explain chemical reactivity of TCA, its molecular stability, as well as electrical and optical properties. According to AIM, NCI, and RDG analysis, TCA and TCA-EtOH complexes mainly have moderate H-bonding.

K e y w o r d s: vibrational spectroscopy, DFT calculation, intermolecular interaction, topological parameters.

1. Introduction

Five-membered sulfur-containing heterocycles, especially thiophene derivatives, have grown in a prominent due to their applications in technology, medicine, supramolecular framework construction, and nonlinear optical materials [1]. Because of this, several scientists have investigated thiophene derivatives [2–9]. In this study, 2-thiophene carboxylic acid (TCA), a biologically active chemical widely used in medicine, is studied. Sarswat *et al.* proposed the computed FT-Raman spectra for this acid [10]. TCA was studied on the Ar surface using the SERS approach [11]. Karthick *et al.* studied the interactions between TCA monomers and dimers by experiments, computations, vibrational, geometric, structural, and docking analyses [4].

In this research, the interactions and spectrum manifestations of TCA and its solutions in ethanol (EtOH) are investigated using Raman and IR spectroscopy, as well as topological analysrs. In addition, quantum chemical parameters such as molecular electrostatic potential surface (MEPS), frontier molecular orbital (FMO), atoms in molecules (AIM), reduced density gradient (RDG), noncovalent interaction (NCI), electron localization functions (ELF), and localized orbital locator (LOL) are investigated in TCA + EtOH complexes. Understanding intermolecular interactions of TCA in various solvents might give useful insights into its prospective uses

C i t a t i o n: Jumabaev A., Khudaykulov B., Koyambo-Konzapa S.-J., Holikulov U., Hushvaktov H., Absanov A., Doroshenko I. Exploring noncovalent interactions of thiophene-2-carboxylic acid in ethanol via vibrational spectroscopy and DFT calculations. *Ukr. J. Phys.* **70**, No. 6, 391 (2025). https://doi.org/10.15407/ujpe70.6.391.

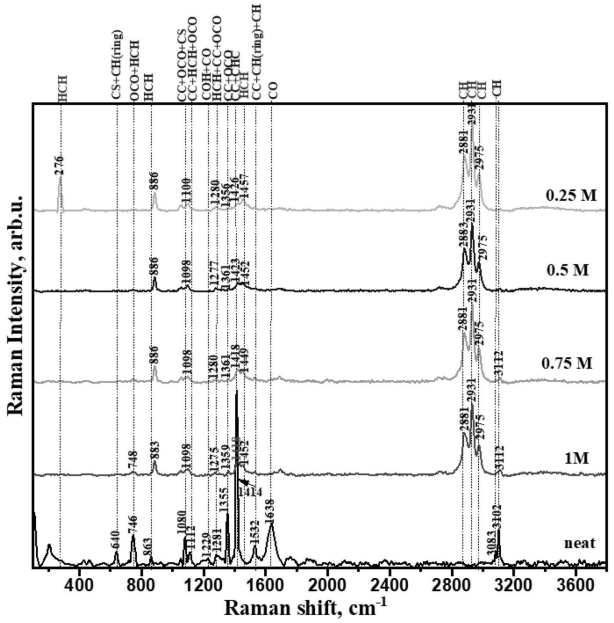

Fig. 1. Raman spectra of TCA in EtOH solutions

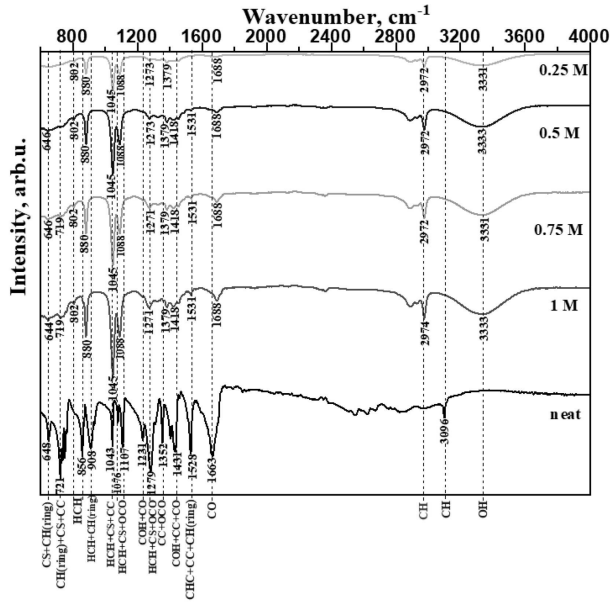

Fig. 2. IR spectra of TCA in EtOH solutions

in drug design, material science, and molecular engineering, highlighting its importance as a scientific research topic.

2. Experimental and Computational Details

Raman spectra of pure 2-thiophene carboxylic acid (TCA) and its solution in ethanol (EtOH) are recorded on a Renishaw Invia Raman spectrometer, and the experimental conditions were detailed in our earlier publications [12, 13]. The IR spectra were acquired using an IRAffinity-1S Fourier spectrometer. The experiments were performed at molarity (M) concentrations, and the spectra were displayed using the Origin 8.5 program [14].

Quantum-chemical simulations were carried out using Gaussian 09W software [15] and the density functional theory (DFT) technique. The global optimal states for different complexes were computed initially with the ABCluster program [16], and then recalculated with the B3LYP/6-311++G(d.p) basis set [17, 18]. Multiwfn 3.8 [19] was used to calculate various topological parameters, which then were displayed using VMD 1.9.3 [20].

3. Results and Discussion

3.1. Vibrational analysis of TCA solutions in EtOH

Vibrational spectroscopy is a useful technique for investigating noncovalent interactions, particularly hydrogen bonds [21–25]. In this work, the vibrational spectra of TCA in EtOH solutions were compared to those in its pure state. Because Raman and IR activities in vibrational spectroscopy rely on polarization and dipole moment changes, respectively, their uses are complimentary. Figures 1, 2 depict the Raman scattering and IR absorption spectra of pure TCA and its solution in EtOH at various molar concentrations. The vibrational frequencies (potential energy distribution, PED analysis) associated with each atom of TCA were similar to the results reported in the literature [4].

The free hydroxyl group absorbs substantially in the 3584–3700 cm^{-1} region, but the creation of intermolecular hydrogen bonds can reduce the O–H stretching frequency in the 3200–3500 cm^{-1} interval [26, 27]. According to Fig. 2, in the IR spectrum of TCA in EtOH solution, the O–H vibration maximum corresponds to 3333 cm^{-1} at a concentration of 1 M, and at 0.25 M, it becomes 3331 cm^{-1}, indicating a red shift due to H-bonding.

Although the weak interaction occurs through C–H during the formation of molecular complexes, they play an essential role in the substance formation [28, 29]. Hetero aromatics such as furans, pyrroles, and thiophenes exhibit C–H stretching bands in the 3100–

3000 cm^{-1} interval. In this scenario (Fig. 1), the maximum of the symmetric C–H stretching vibration band of pure TCA corresponds to 3102 cm^{-1} in Raman, but in a 1M EtOH solution, the maximum is 3112 cm^{-1}, with a blue shift of 10 cm^{-1} was detected. The low-intensity maximum at 3083 cm^{-1} indicates asymmetric C–H stretching, which was not found in the EtOH solution. The C–H stretching vibrations of EtOH can be seen by the 2881, 2931, and 2975 cm^{-1} (red lines), which did not alter, as the EtOH concentration decreased.

In the IR spectrum (Fig. 2), the C–H stretching maximum of pure TCA corresponds to 3096 cm^{-1}, the C–H stretching maximum of EtOH in a solution of 1 M corresponds to 2974 cm^{-1}, and when the concentration is reduced to 0.25 M, it is red-shifted to 2972 cm^{-1}.

The C=O stretching vibration is typically regarded as a distinctive frequency for carboxylic acids, and in pure TCA this maximum occurs at 1638 cm^{-1} in Raman, with a relatively small intensity in solution (Fig. 1). The characteristic absorption bands of C=O stretching vibrations of acids tend to be high in intensity and located in the 1800–1690 cm^{-1} region. In TCA, the conjugation of C=O and C=C bonds increases the frequency of carbonyl stretching. The C=O stretching vibration maximum in IR is 1663 cm^{-1}, but when dissolved in EtOH, it shifts to 1688 cm^{-1}.

Figure 1 shows that in pure TCA, the CC + CHC and HCH vibrations are at 1418 cm^{-1} and 863 cm^{-1}, respectively, whereas in the solution they are blue-shifted to 1426 cm^{-1} and 886 cm^{-1}. The CC + OCO + CS vibrational system is shifted from 1080 to 1100 cm^{-1}. The other bands did not exhibit significant change. Figure 2 shows that in the IR spectra, the CHC + CC + CH ring vibrations are blue-shifted from 1528 to 1531 cm^{-1}, whereas the COH + CC + CO band is red-shifted from 1431 to 1418 cm^{-1}. Furthermore, a red shift was seen for the vibrations HCH + CS + OCO; HCH + CS + CC; HCH + CH(ring); HCH; CH(ring) + CS + CC, and CS + CH(ring) compared to the pure state, whereas a blue shift was detected for HCH + CS + CC one.

3.2. Molecular electrostatic potentials surface (MEPS)

MEPS analysis is important for understanding the electrophilic (negative) and nucleophilic (positive) aspects of chemical processes that include intramolecular charge transfer, hydrogen bonding, and other interactions [30–34]. MEPS mapping is also a method for calculating and mapping electrostatic potential of a molecule at various locations on its surface. Color codes make distinctions between electrophilic and nucleophilic localizations. Positive (nucleophilic) regions, which lack electrons, are represented by blue; negative (electrophilic) regions, which have an abundance of electrons, are represented by red; and neutral regions are represented by green.

Fig. 3 depicts MEPS color code categorization. Electrostatic potential increases in the following order: red < orange < yellow < green < blue. The MEPS map demonstrates that the oxygen atom in TCA's carboxyl and hydroxyl groups has a negative potential, as the red indicates the electrophilic region of the molecule, which has the most negative charge. The blue color around the hydrogen atoms shows the nucleophilic moiety's positive charge, whereas the yellow denotes a region with slightly more electrons. The MEPS diagram is also presented for the dimer, trimer, and TCA complexes with EtOH. The potential energies for the monomer, dimer, and trimer are $5.641e^{-2} \div 5.641e^{-2}$ a.u., $-3.660e^{-2} \div 3.660e^{-2}$ a.u., and $-4.302e^{-2} \div 4.302e^{-2}$ a.u., respectively. The diagram shows that when the monomer progresses to dimer and trimer, the oxygen in carboxyl and hydroxyl groups (red) forms a complex and the negative electropotential decreases (changes to yellow). The potential value declined as the complex size increased. The TCA-EtOH complex has the highest MEPS potential value ($-4.302e^{-2} \div 4.302e^{-2}$ a.u.) among all TCA-$(EtOH)_m$ (m = 1–4) complexes. As the EtOH number in the complex grew, the potential value declined, but for TCA-$(EtOH)_4$, it increased again ($-4.217e^{-2} \div 4.217e^{-2}$ a.u.). When we look at the MEPS, we can see that the TCA and EtOH oxygen atoms establish bonds via the negative electron potential regions, which are highlighted in red.

3.3. Frontier molecular orbital (FMO) analysis

Frontier molecular orbitals (HOMO-LUMO) are commonly used to explain molecular chemical reactivity, stability, electrical and optical characteristics [35]. These orbitals are the outermost borders of a mole-

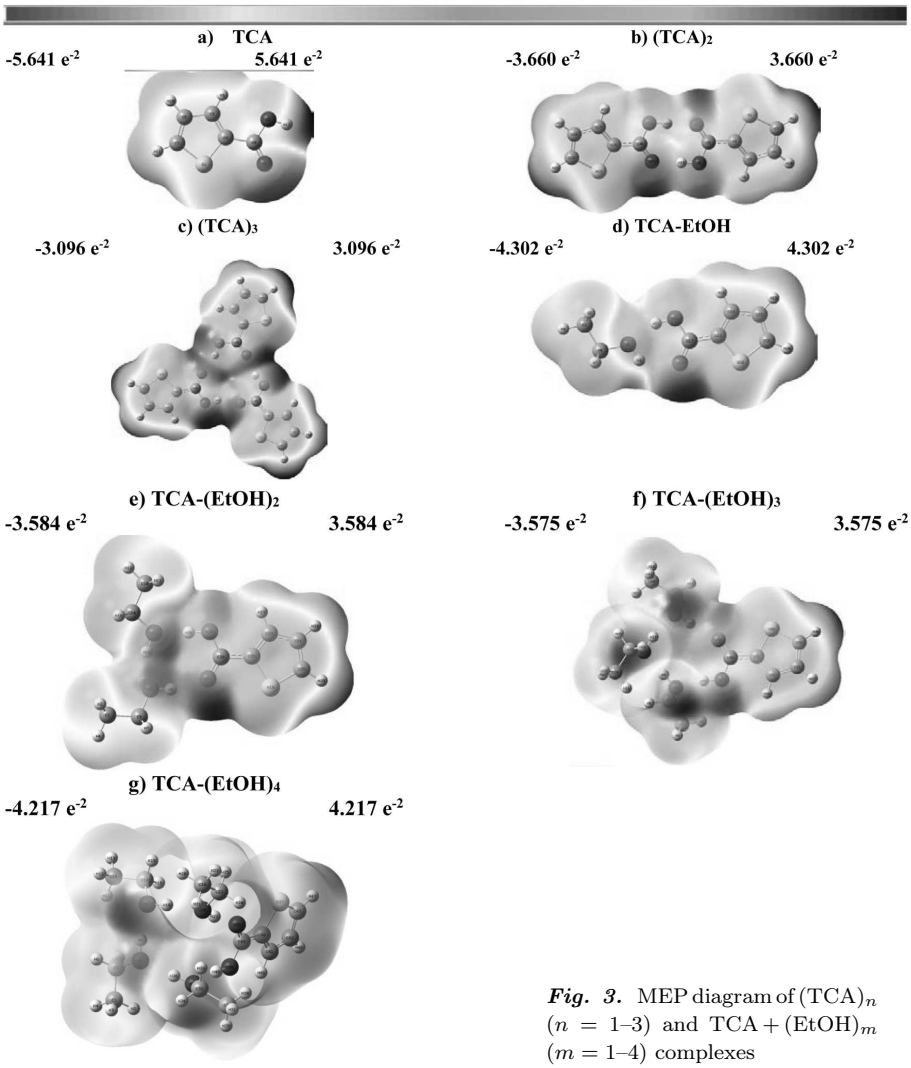

Fig. 3. MEP diagram of $(\mathrm{TCA})_n$ (n = 1–3) and $\mathrm{TCA}+(\mathrm{EtOH})_m$ (m = 1–4) complexes

cule's electronic structure and play an important role in many chemical reactions, particularly those requiring electron transfers. The HOMO plays an essential role in electron-donating or nucleophilic processes. A molecule with a moderately high energy HOMO is often a valuable electron donor and may readily engage in oxidation or nucleophilic processes [13]. Figure 4 depicts the HOMO-LUMO visualization and energy gap (ΔE).

The energy difference between HOMO and LUMO is known as the energy gap. Table 1 lists the FMO parameters estimated using energy gap values, including electrophilicity index of the complexes, chemical hardness, chemical softness, and electronegativity. HOMO has an energy value (E_{HOMO}) of –7.1868 eV, whereas LUMO has an energy value (EW_{LUMO}) of –2.0044 eV. The energy gap value is −5.1824 eV, indicating the compound's reactivity.

The ΔE of TCA dimer and trimer are 5.0646 eV and 5.0861 eV, respectively. The ΔE value for $\mathrm{TCA}+(\mathrm{EtOH})_m$ (m = 1–4) complexes increased from 5.1915 eV to 5.2010 eV as the number of EtOH increased, indicating an increase in reactivity. The TCA monomer, dimer, and trimer have η values of 2.5912, 2.5323, and 2.5430 a.u., respectively. The values for the $\mathrm{TCA}+(\mathrm{EtOH})_m$ (m = 1–4) complexes were 2.5958÷2.6005 a.u. (raised) in terms of ΔE. The TCA monomer, dimer, and trimer had μ values of

4.5956, 4.6134, and 4.5123 a.u., respectively. The μ values of TCA + $(EtOH)_m$ (m = 1–4) complexes declined and then rose with increasing EtOH numbers.

3.4. Atoms in molecules (AIM) analysis

Atoms in molecules (AIM) analysis is commonly used to evaluate noncovalent interactions in molecular systems, namely intra- and intermolecular H-bonds [36]. Due to the electron density, a bonding path is formed between two interacting atoms, resulting in critical points (CPs) in the electron density. At such points, the electron density gradient disappears [37]. Electron density topological analysis confirms the presence of hydrogen bonds and other interactions in molecular complexes. Table 2 shows the topological parameters for the $(TCA)_n (n = 1–3)$ and TCA + $(EtOH)_m$ (m = 1–4) complexes, including electron density $\rho(r)$, electron density Laplacian $\nabla^2\rho(r)$, energy density $H(r)$, Lagrangian kinetic energy density $G(r)$, and potential energy density $V(r)$ in CPs. These parameters provide valuable information about H-bonding. According to [38], the hydrogen bonding interaction can be calculated as shown below:

$\nabla^2\rho(r) > 0, \quad H(r) > 0\, va\, E_{HB} <$

< 12 kcal/mol–weak H-bond;

$\nabla^2\rho(r) > 0, \quad H(r) < 0\, va\, 12 < E_{HB} <$

< 24 kcal/mol–average H-bond;

$\nabla^2\rho(r) < 0, \quad H(r) < 0\, va\, E_{HB} >$

> 24 kcal/mol–strong H-bond.

Table 2 shows that the electron density Laplacians ($\nabla^2\rho(r)$) for the TCA dimer, trimer and TCA-EtOH complexes are positive, with values ranging from 0.13953 to 0.14028 a.u. and from 0.07738 to 0.14932 a.u. The energy densities (H(r)) for the critical points in the following complexes: $(TCA)_2$; TCA-EtOH (8(O) ... 21(H)); TCA-$(EtOH)_2$ (17(O) ... 30(H)); TCA-$(EtOH)_3$ (8(O) ... 39(H), 9(H) ... 26(O) and 27(H) ... 17(O)) and TCA-$(EtOH)_4$ (35(O) ... 48(H), 36(H) ... 8(O), 9(H) ... 17(O) and 26(O) ... 18(H)) take a negative value, indicating moderate H-bonding and weak H-bonding or van der Waals interactions at the remaining critical points [38, 39] (Fig. 5).

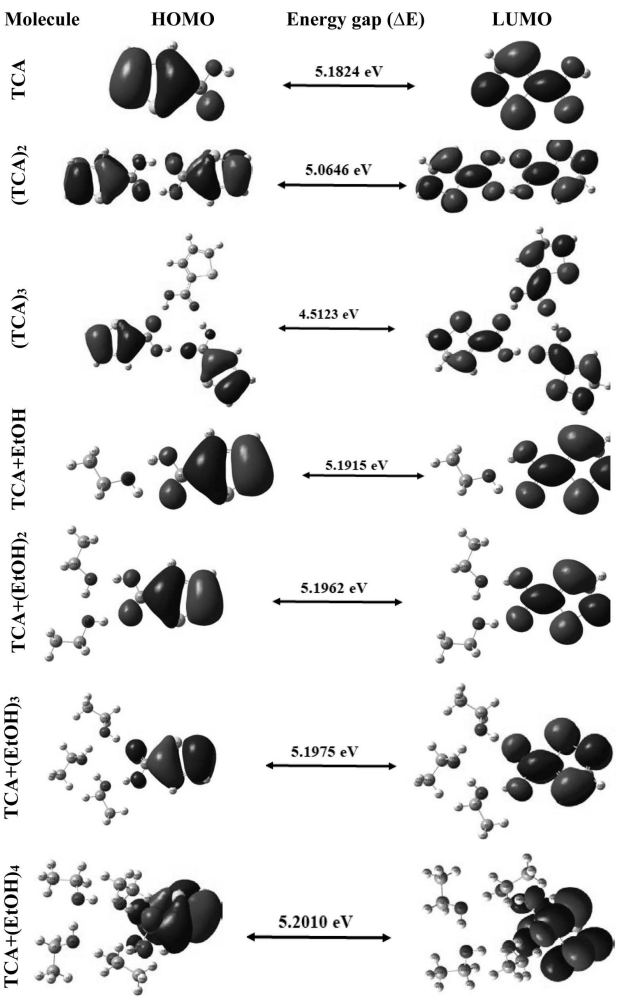

Fig. 4. FMO diagrams of $(TCA)_n$ (n = 1–3) and TCA + + $(EtOH)_m$ (m = 1–4) complexes

The hydrogen bond energy was calculated using the formula: $E_{HB} = -V(r)/2$ [13]. $V(r)$ represents the potential energy density at hydrogen bonding's critical points. If the energy density at the CP is negative, the bond is covalent; if it is positive, the bond is electrostatic. All complexes in Fig. 5 are bonded by weak H-bonds, which are typical of electrostatic interactions. The bond lengths in the TCA-$(EtOH)_4$ complex (33(H) ... 26(O) are at least 2.1 Å. This verifies the presence of weak mutual H-bonds in these complexes, which are also known as van der Waals in-

Table 1. **FMO related parameters of $(TCA)_n$ ($n = 1$–3) and $TCA + (EtOH)_m$ ($m = 1$–4) complexes**

Parameters	E_{HOMO}, eV	E_{LUMO}, eV	$E_{LUMO} - E_{HOMO}$	Global hardness $\eta = (E_{LUMO} - E_{HOMO})/2$	Chemical potential $\mu = (E_{LUMO} + E_{HOMO})/2$	Global electrophilic index $\omega = \mu^2/2\eta$
TCA	–7.1868	–2.0044	5.1824	2.5912	4.5956	4.0752
$(TCA)_2$	–7.1457	–2.0811	5.0646	2.5323	4.6134	4.2025
$(TCA)_3$	–7.0554	–1.9693	5.0861	2.5430	4.5123	4.0033
TCA + EtOH	–7.0138	–1.8223	5.1915	2.5958	4.4181	3.7598
$TCA + (EtOH)_2$	–6.9733	–1.7771	5.1962	2.5981	4.3752	3.6840
$TCA + (EtOH)_3$	–6.9850	–1.7875	5.1975	2.5988	4.3862	3.7016
$TCA + (EtOH)_4$	–6.9877	–1.7867	5.2010	2.6005	4.3872	3.7007

Table 2. **Topological parameters of $(TCA)_n$ ($n = 1$–3) and $TCA + (EtOH)_m$ ($m = 1$–4) complexes**

Name of clusters	H-bonds	Bond length r, Å	Density of all electrons $\rho(r)$	Lagrangian kinetic energy $G(r)$	Potential energy density $V(r)$	Energy density $H(r)$	Laplacian of electron density $\nabla^2\rho(r)$	Hydrogen bond energy E_{HB}, kcal/mol
$(TCA)_2$	15(O) ... 12(H)	1.65996	0.04829	0.04049	–0.04610	–0.00561	0.13953	15.15
	24(H) ... 3(O)	1.65996	0.04829	0.04049	–0.04610	–0.00561	0.13953	15.15
$(TCA)_3$	36(H) ... 3(O)	1.71788	0.03637	0.03463	–0.03419	0.00044	0.14028	10.87
	12(H) ... 15(O)	1.71869	0.03619	0.03453	–0.03402	0.00052	0.14018	10.67
	27(O) ... 24(H)	1.71781	0.03629	0.03459	–0.03411	0.00047	0.14023	10.70
TCA-EtOH	9(H) ... 12(O)	2.05318	0.02135	0.01743	–0.01552	0.00191	0.07738	4.87
	8(O) ... 21(H)	1.75801	0.03608	0.03240	–0.03266	–0.00025	0.12859	10.25
$TCA\text{-}(EtOH)_2$	9(H) ... 21(O)	1.83429	0.03026	0.02663	–0.02500	0.00163	0.11305	7.84
	8(O) ... 18(H)	1.77812	0.03423	0.03119	–0.03060	0.00059	0.12712	9.60
	17(O) ... 30(H)	1.65418	0.04781	0.04128	–0.04655	–0.00527	0.14402	14.61
$TCA\text{-}(EtOH)_3$	8(O) ... 39(H)	1.61448	0.05536	0.04574	–0.05508	–0.00935	0.14556	17.28
	9(H) ... 26(O)	1.71512	0.04345	0.03661	–0.04000	–0.00339	0.13287	12.55
	27(H) ... 17(O)	1.73810	0.04042	0.03481	–0.03672	–0.00192	0.13158	11.52
	30(O) ... 18(H)	1.80313	0.03071	0.02837	–0.02640	0.00197	0.12132	8.28
$TCA\text{-}(EtOH)_4$	35(O) ... 48(H)	1.59189	0.05835	0.04831	–0.05929	–0.01098	0.14932	18.60
	36(H) ... 8(O)	1.72391	0.04129	0.03582	–0.03809	–0.00228	0.13417	11.95
	33(H) ... 26(O)	2.75735	0.00582	0.00380	–0.00333	0.00047	0.01706	1.04
	9(H) ... 17(O)	1.76274	0.03835	0.03228	–0.03366	–0.00138	0.12362	10.56
	39(O) ... 27(H)	1.79098	0.03261	0.02959	–0.02834	0.00125	0.12336	8.89
	26(O) ... 18(H)	1.76410	0.03783	0.03243	–0.03343	–0.00100	0.12569	10.49

teractions. The remaining bond lengths imply moderate H-bonding.

3.5. Non-covalent interaction (NCI) and reduced density gradient (RDG)

RDG and NCI studies are recent approaches for characterizing weak intermolecular interactions [34, 36, 40]. The NCI index is used to define intermolecular interactions and determine the type of weak interactions. The NCI index, based on the reduced density gradient (RDG), provides additional information when analyzing noncovalent interactions. The reduced density gradient (RDG) is a fundamental dimensionless variable consisting of the density and its

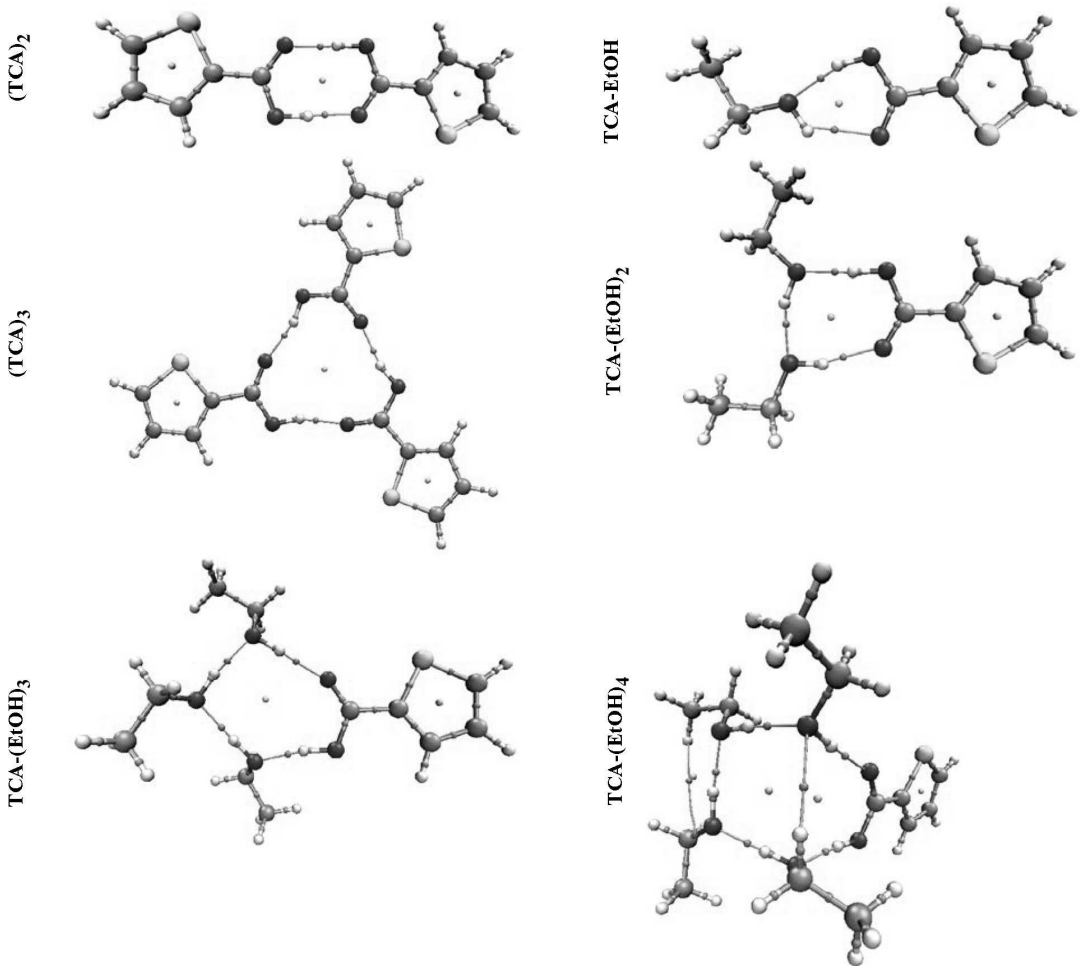

Fig. 5. The AIM analysis for $(\mathrm{TCA})_n (n = 1–3)$ and $\mathrm{TCA} + (\mathrm{EtOH})_m$ $(m = 1–4)$ complexes

first derivative, and is expressed by formula [36]:

$$\mathrm{RDG}(r) = \frac{1}{2(3\pi^2)}^{1/3} \frac{|\nabla\rho(r)|^{4/3}}{\rho(r)}.$$

The electron density of the $\mathrm{sign}\,(\lambda_2)\rho$ relative to the RDG reveals the nature and extent of intermolecular interactions. In molecular systems, blue denotes mutual attraction while red implies repulsion. $\mathrm{sign}(\lambda_2)\rho$ plays a crucial role in anticipating the type of an interaction. For instance, $\mathrm{sign}\,(\lambda_2)\rho < 0$ suggests repulsive forces between bonded atoms, whereas $\mathrm{sign}\,(\lambda_2)\rho > 0$ implies repulsive forces between unbonded atoms.

The RDG scatter plot for the complexes is presented on the right side of Fig. 6. According to the expression at the top of the diagram, red signifies strong repulsive forces (steric or cyclic effect), blue indicates H-bonding, and green shows the presence of van der Waals interactions. According to the results, the red markings between the TCA dimer rings suggest the presence of a cyclic effect (Fig. 6, *a*). Internal van der Waals interactions exist between the C–H group and the O–H group of the ring, as well as between the O atoms of C=O and S. It can also be seen from the RDG scattering plot on the right side of Fig. 6, *a* that the scattering is mainly in the range of $\mathrm{sign}\,(\lambda_2)\,\rho$, which is –0.01 and represents van der Waals interaction. The scattered part at 0.01 and 0.04 is in red, representing the cyclic effect of the ring. The blue scattered part at –0.05 represents the H-bonding in the form of O–H ... C=O. The identical condition occurs in the trimer (Fig. 6, *b*). Fig. 6, *c* depicts the TCA-

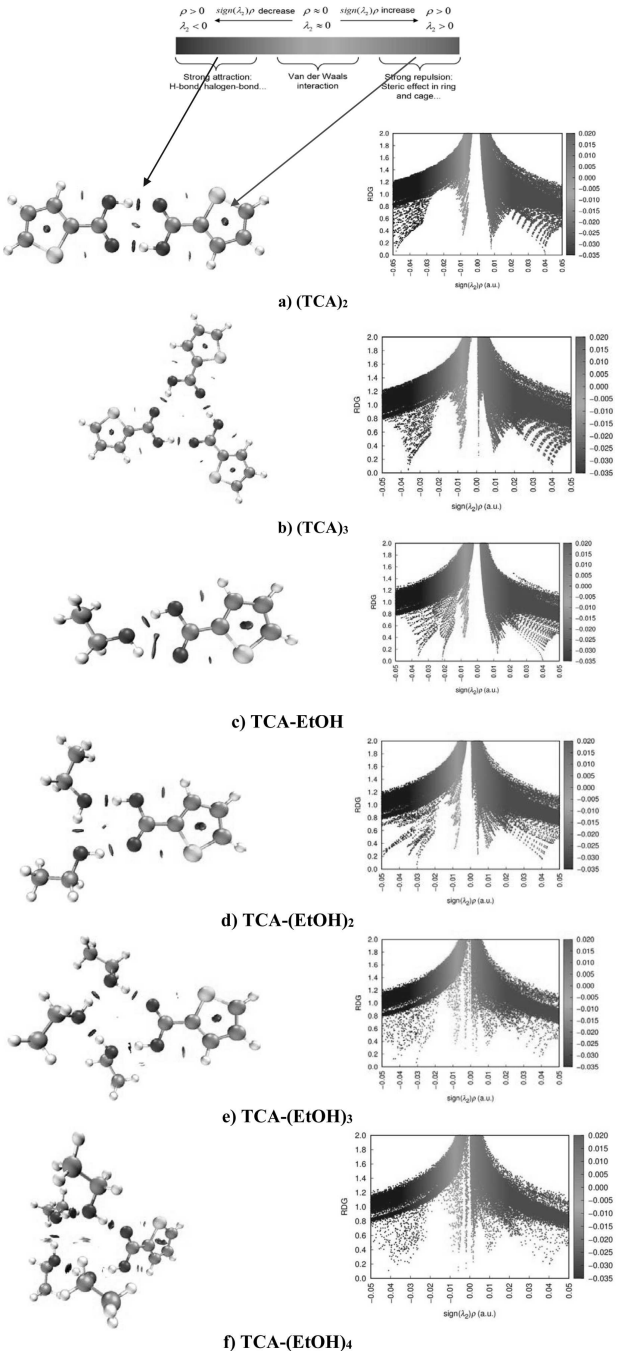

Fig. 6. NCI and RDG analyses for $(\mathrm{TCA})_n$ (n = 1–3) and $\mathrm{TCA} + (\mathrm{EtOH})_m$ (m = 1–4) complexes

EtOH heterodimer. H-bonds of the form O–HC=O and O–HO exist between the carbonyl and hydroxyl groups of TCA and the EtOH atoms, corresponding to sign $(\lambda_2)\,\rho$ values of –0.35 and –0.02, respectively, representing H-bonding and van der Waals interactions in the RDG scattering plot.

According to Fig. 6, C=O, O–H and C–H groups of TCA interact with the EtOH atoms, resulting in greater shifts in the stretching vibration bands of these groups in the experiment. In general, H-bonding dominates in TCA dimers, trimers, and its complexes with EtOH.

3.6. ELF and LOL analyses

Electron localization function (ELF) and localized orbital locator (LOL) investigations are often used to describe chemical bonds in atomic and molecular systems, as well as to detect electron-containing locations. The chemical formulae of ELF and LOL are determined by the kinetic energy density $D(r)$, among other factors [41]. However, ELF is determined by electron pair density. LOL simply represents the gradient of localized orbits and is used when localized orbits overlap. The value of ELF, $\tau(r)$, spans from 0.0 to 1.0, with high values between 0.5 and 1.0 reflecting regions having bonding and nonbonding localized electrons, and lesser values (<0.5) indicating places where electron delocalization is projected. The LOL, $\eta(r)$ with large values (>0.5) showed places where the density of electrons is dominated by their position [42–44]. Pauli repulsion occurs owing to excess energy density, which is the region of space used to determine the likelihood of opposing spin-pair or single electron behavior. The stronger the Pauli attraction of ELF, the closer it is to one, whereas the Pauli repulsion of ELF is closer to zero. The ELF values are colour coded as follows. Red color indicates a high ELF (0.8–1), whereas blue indicates a low ELF value. Green signifies the transition between red and blue via yellow [13]. The 2D ELF and LOL images of $(\mathrm{TCA})_n (n = 1–3)$ and $\mathrm{TCA} + (\mathrm{EtOH})_m$ (m = 1–4) complexes in three coordinate planes are displayed in Figs. 7–13. The ELF revealed that the C and S atoms in the ring appear blue, whereas the H atoms appear red. The LOL study showed the chemical bonding behavior of the molecule supplied by atoms, as well as the maximum localized orbital, i.e. overlap, that occurs owing to orbital gradient. The ring carbon in the ring system is depicted in blue color circles, and the bond critical point is marked by red color in some of the ring

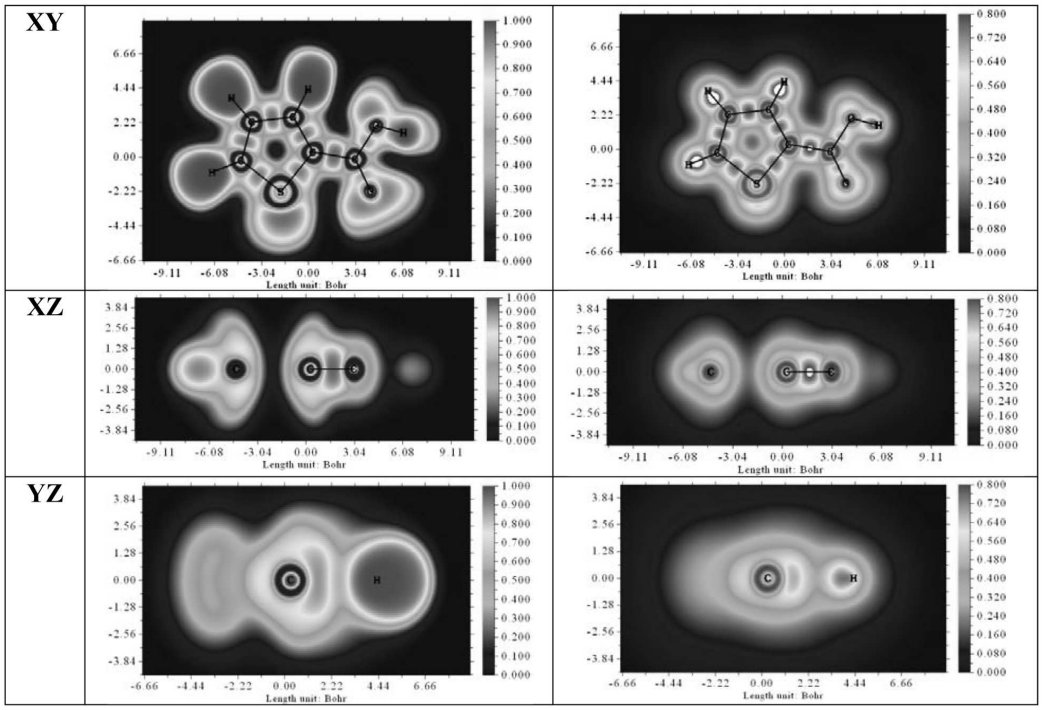

Fig. 7. ELF (left) and LOL (right) maps of the TCA molecule

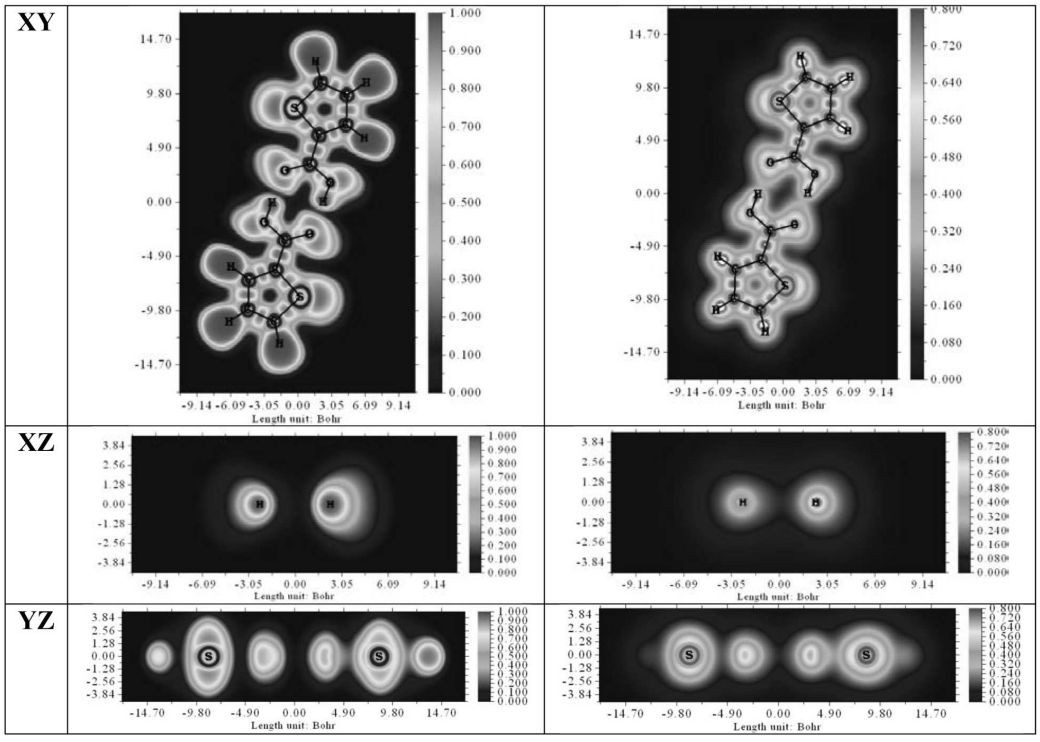

Fig. 8. ELF (left) and LOL (right) maps of the $(TCA)_2$ complex (dimer)

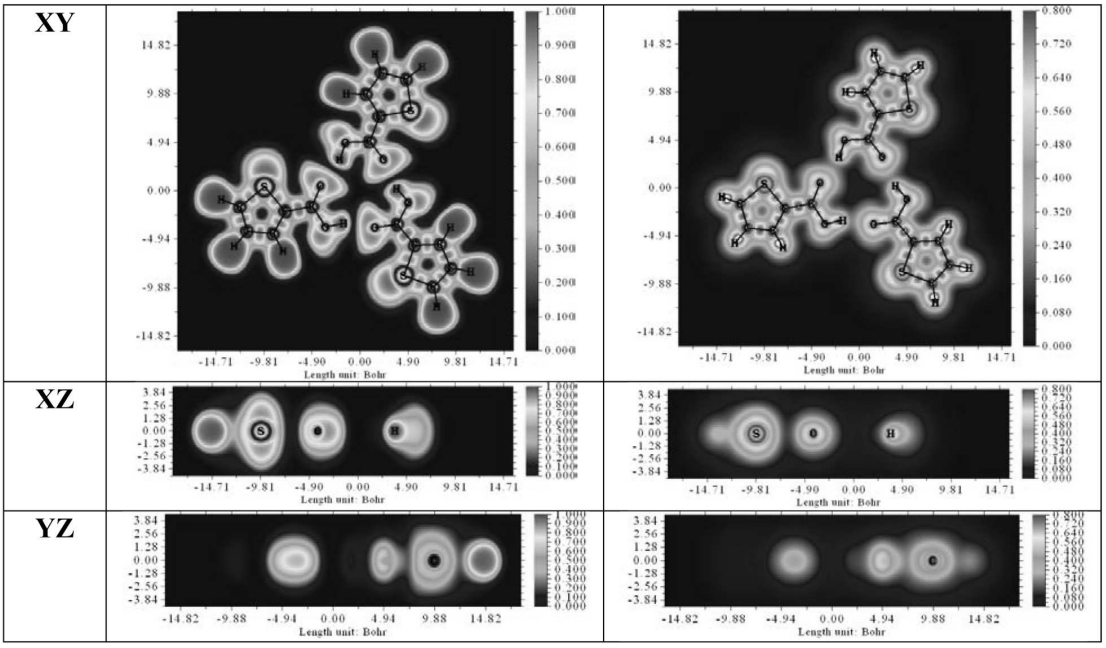

Fig. 9. ELF (left) and LOL (right) maps of the $(TCA)_3$ complex (trimer)

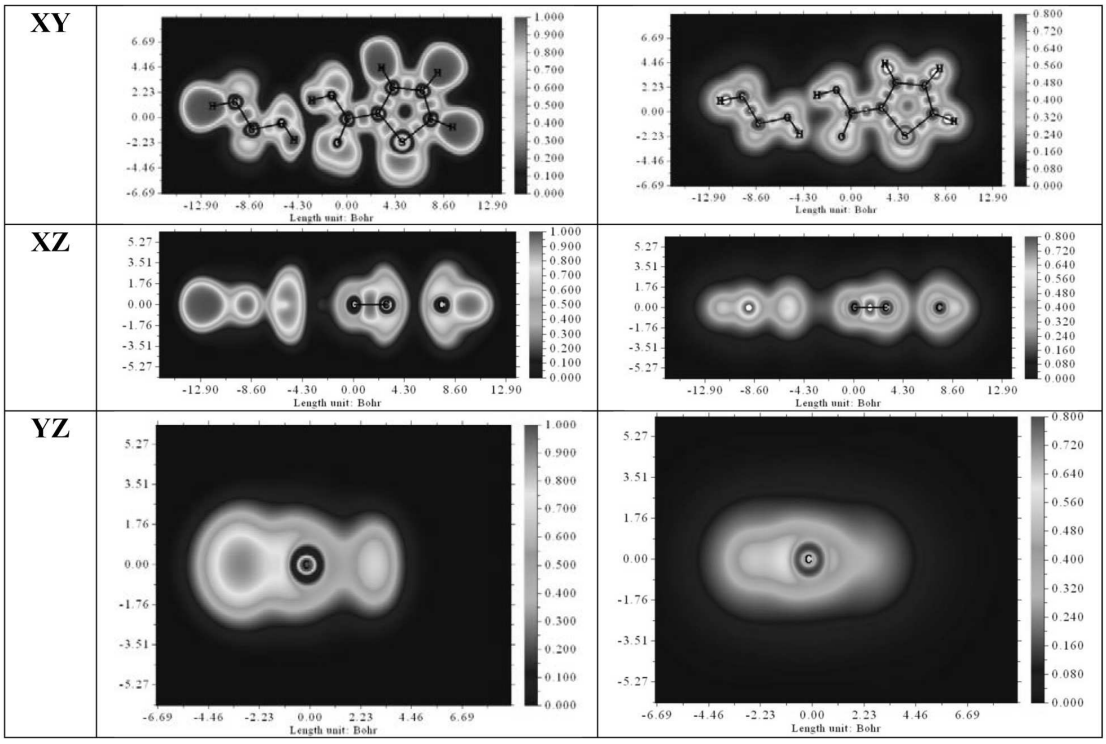

Fig. 10. ELF (left) and LOL (right) maps of the TCA + EtOH complex

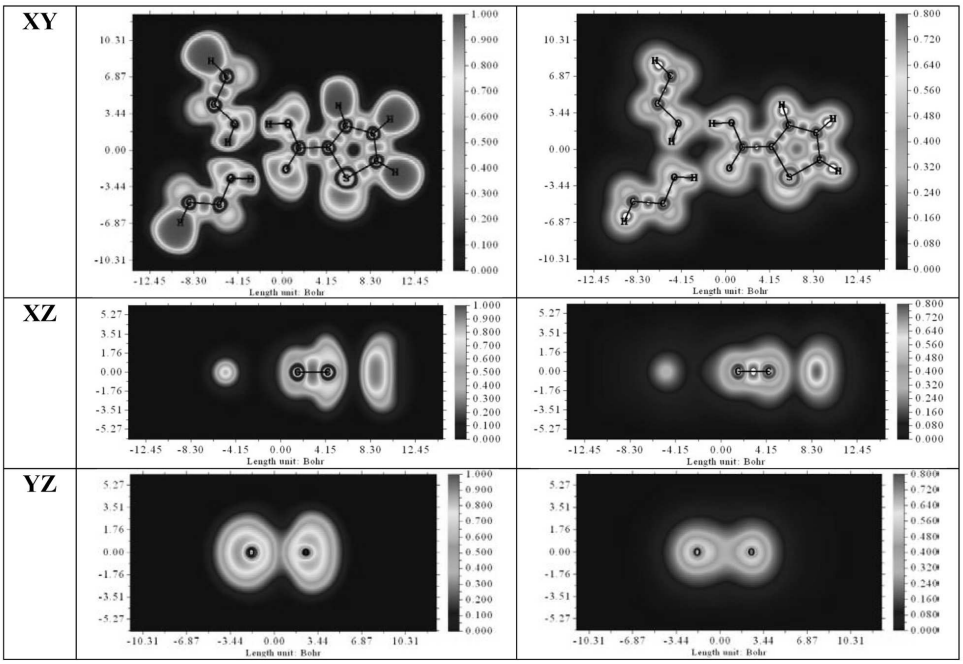

Fig. 11. ELF (left) and LOL (right) maps of the TCA + $(EtOH)_2$ complex

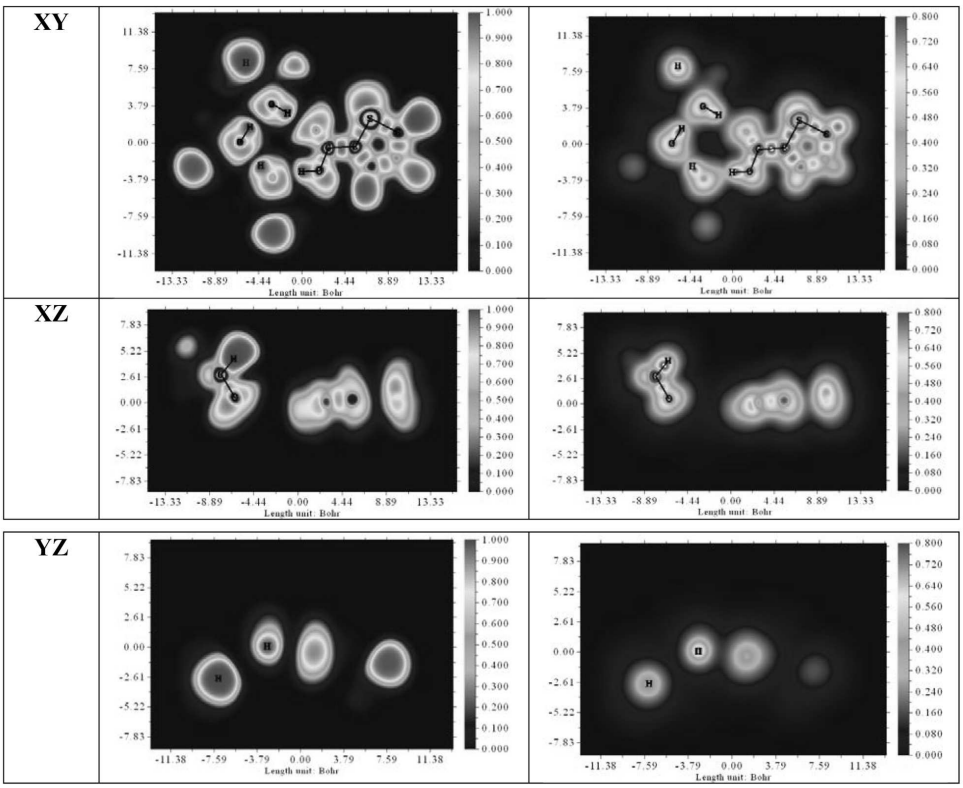

Fig. 12. ELF (left) and LOL (right) maps of the TCA + $(EtOH)_3$ complex

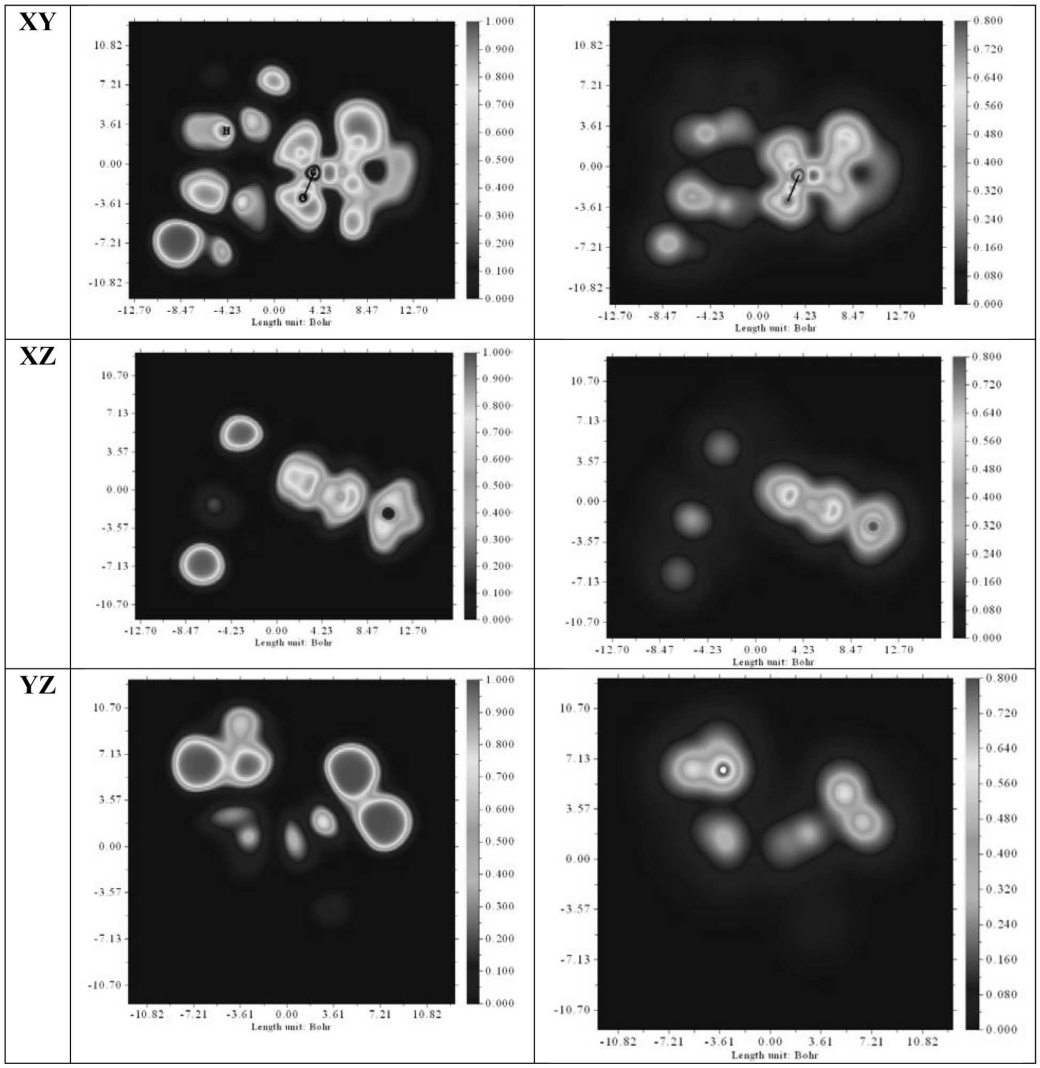

Fig. 13. ELF (left) and LOL (right) maps of the TCA + $(EtOH)_4$ complex

carbon atoms and carbon atoms coupled to oxygen, while delocalization is also apparent in yellow color in Figs. 7–13.

4. Conclusion

The present work is a spectroscopic and quantum computational analysis of thiophene-2-carboxylic acid (TCA) and its ethanol solutions. The complexes are calculated by DFT method with B3LYP technique and 6-311++G(d, p) basis set. The vibrational spectra are collected in the range of 400–4000 cm^{-1}. In general, red or blue shifts were seen in the O–H, C=O and C–H stretching bands in TCA solution with EtOH. This shows that H-bonding or van der Waals interactions might be present in the solutions. However, the observed ring C–H stretching vibrational frequencies in TCA molecules shifted towards higher frequencies, which can be attributed to the existence of intra- and intermolecular interactions, as well as hyper-conjugation interactions. Quantum-chemical calculations were conducted to verify this assumption. According to the MEPS study, the potential in the solvents is created by the negative electron parts of TCA, and EtOH oxygen atoms, which are highlighted in red. The HOMO → LUMO tran-

sition indicates an energy transfer from the aromatic heterocyclic ring. The energy gap evaluates the kinetic stability of molecules. A molecule with a narrow border orbital gap is highly polarizable, indicating strong chemical reactivity but low kinetic stability. When AIM, NCI, and RDG studies were used to assess noncovalent interactions, it is discovered that TCA and TCA-EtOH complexes mostly had moderate H-bonding. Furthermore, H-bonds were formed between the C=O, O–H and C–H groups of TCA and the EtOH atoms, resulting in more shifts in the stretching vibration bands of the these groups in the experiment. In general, H-bonding of TCA dimers, trimers, and in EtOH solutions predominated. The chemical bonds and electron positions in the complexes were color-coded using electron localization function (ELF) and localized orbital locator (LOL) analyses.

This work was supported by Project No. FZ-20200929385, Ministry of Higher Education, Science and Innovation of the Republic of Uzbekistan.

1. F. Cagnin, E.E. Castellano, M.R. Davolos. Synthesis and structural characterization of a new polymeric zinc(II) complex with thiophene-2-carboxylic acid. *J. Coord. Chem.* **63**, 2278 (2010).
2. V. Hernández, F.J. Ramírez, J. Casado, F. Enríquez, J.J. Quirante, J.L. Navarrete. Ab initio RHF 6-31G** theoretical study of thiophene derivatives: 2-methylthiophene and 3-methylthiophene. *J. Mol. Struct.* **410**, 311 (1997).
3. T. Kupka, R. Wrzalik, G. Pasterna, K. Pasterny. Theoretical DFT and experimental Raman and NMR studies on thiophene, 3-methylthiophene, and selenophene. *J. Mol. Struct.* **616**, 17 (2002).
4. T. Karthick, V. Balachandran, S. Perumal. Spectroscopic investigations, molecular interactions, and molecular docking studies on the potential inhibitor "thiophene-2-carboxylic acid". *Spectrochim. Acta A Mol. Biomol. Spectrosc.* **141**, 104 (2015).
5. G.D. Fleming, R. Koch, M.C. Vallete. Theoretical study of the *syn* and *anti* thiophene-2-aldehyde conformers using density functional theory and normal coordinate analysis. *Spectrochim. Acta A Mol. Biomol. Spectrosc.* **65**, 935 (2006).
6. V. Balachandran, A. Janaki, A. Nataraj. Theoretical investigations on molecular structure, vibrational spectra, HOMO, LUMO, NBO analysis, and hyperpolarizability calculations of thiophene-2-carbohydrazide. *Spectrochim. Acta A Mol. Biomol. Spectrosc.* **118**, 321 (2014).
7. L.L. Gladkov, S.V. Gaponenko, E.V. Shabunya-Klyachkovskaya, A.N. Shimko, E.S. Al-Abdullah, A.A. El-Emam. Vibrational spectroscopy of N′-(adamantan-2-ylidene) thiophene-2-carbohydrazide, a potential antibacterial agent. *Spectrochim. Acta Part A Mol. Biomol. Spectrosc.* **128**, 874 (2014).
8. S. Abbas, M. Hussain, S. Ali, M. Parvez, A. Raza, A. Haider, J. Iqbal. Structural, enzyme inhibition, antibacterial and DNA protection studies of organotin (IV) derivatives of thiophene-2-carboxylic acid. *J. Organomet. Chem.* **724**, 255 (2013).
9. T. Nasr, S. Bondock, S. Eid. Design, synthesis, antimicrobial evaluation and molecular docking studies of some new thiophene, pyrazole and pyridone derivatives bearing sulfisoxazole moiety. *Eur. J. Med. Chem.* **84**, 491 (2014).
10. P.K. Sarswat, A. Sathyapalan, Y. Zhu, M.L. Free. Design, synthesis, and characterization of TPA-thiophene-based amide or imine functionalized molecule for potential optoelectronic devices. *J. Theor. Appl. Phys.* **7**, 1 (2013).
11. U.K. Sarkar. A pH-dependent SERS study of thiophene-2-carboxylic acid adsorbed on Ag-sols. *Chem. Phys. Lett.* **374**, 341 (2003).
12. A. Jumabaev, H. Hushvaktov, B. Khudaykulov, A. Absanov, M. Onuk, I. Doroshenko, L. Bulavin. Formation of hydrogen bonds and vibrational processes in dimethyl sulfoxide and its aqueous solutions: Raman spectroscopy and ab initio calculations. *Ukr. J. Phys.* **68**, 375 (2023).
13. A. Jumabaev, S.J. Koyambo-Konzapa, H. Hushvaktov *et al.* Intermolecular interactions in water and ethanol solution of ethyl acetate: Raman, DFT, MEP, FMO, AIM, NCI-RDG, ELF, and LOL analyses, *J. Mol. Model.* **30**, 349 (2024).
14. J.G. Moberly, M.T. Bernards, K.V. Waynant. Key features and updates for Origin 2018. *J Cheminform* **10**, 5 (2018).
15. M.J. Frisch *et al.* Gaussian 09, Revision D.1, Gaussian Inc., Wallingford, 2009.
16. J. Zhang, M. Dolg. ABCluster: The artificial bee colony algorithm for cluster global optimization. *Phys. Chem. Chem. Phys.* **17**, 24173 (2015).
17. A.D. Becke. Density-functional thermochemistry. III. The role of exact exchange. *J. Chem. Phys.* **98**, 5648 (1993).
18. C. Lee, W. Yang, R.G. Parr. Development of the Colle–Salvetti correlation energy formula into a functional of the electron density. *Phys. Rev. B Condens. Matter.* **37**, 785 (1998).
19. T. Lu, F. Chen. Multiwfn: A multifunctional wavefunction analyzer. *J. Comput. Chem.* **33**, 580 (2012).
20. W. Humphrey, A. Dalke, K. Schulten. VMD: Visual molecular dynamics. *J. Mol. Graph.* **14**, 33 (1996).
21. A. Jumabaev, B. Khudaykulov, I. Doroshenko, H. Hushvaktov, A. Absanov. Raman and ab initio study of in-

termolecular interactions in aniline. *Vib. Spectrosc.* **122**, 103422 (2022).
22. H. Hushvaktov, B. Khudaykulov, A. Jumabaev, I. Doroshenko, A. Absanov, G. Murodov. Study of formamide molecular clusters by Raman spectroscopy and quantum-chemical calculations. *Mol. Cryst. Liq. Cryst.* **749**, 124 (2022).
23. O. Mishchuk, I. Doroshenko, V. Sablinskas, V. Balevicius. Temperature evolution of cluster structure in *n*-hexanol, isolated in Ar and N_2 matrices and in condensed states. *Struct. Chem.* **27**, 243 (2016).
24. H. Hushvaktov, F. Tukhvatullin, A. Jumabaev, U. Tashkenbaev, A. Absanov, B. Hudoyberdiev, B. Kuyliev. Raman spectra and ab initio calculation of a structure of aqueous solutions of methanol. *J. Mol. Struct.* **1131**, 25 (2017).
25. G.A. Pitsevich, I.Yu. Doroshenko, V.Ye. Pogorelov, E.N. Kozlovskaya, T. Borzda, V. Sablinskas, V. Balevicius. Long-wave Raman spectra of some normal alcohols. *Vibr. Spectrosc.* **72**, 26 (2014).
26. V. Balevicius, V. Sablinskas, I. Doroshenko, V. Pogorelov. Propanol clustering in argon matrix: 2D FTIR correlation spectroscopy. *Ukr. J. Phys.* **56**, 855 (2011).
27. I. Doroshenko, V. Pogorelov, V. Sablinskas, V. Balevicius. Matrix-isolation study of cluster formation in methanol: O-H stretching region. *J. Mol. Liq.* **157**, 142 (2010).
28. E. Mrazkova, P. Hobza. Hydration of sulfo and methyl groups in dimethyl sulfoxide is accompanied by the formation of red-shifted hydrogen bonds and improper blue-shifted hydrogen bonds: An ab initio quantum chemical study. *J. Phys. Chem. A* **107**, 1032 (2003).
29. M. Lu, H. Haoran, W. Congmin, X. Yingjie, H. Shijun. Prediction of vapor-liquid equilibria data from C–H band shifts of Raman spectra and activity coefficients at infinite dilution in some aqueous systems. *Ind. Eng. Chem. Res.* **44**, 6883 (2005).
30. T. Lu, F. Chen. Quantitative analysis of molecular surface based on improved marching tetrahedra algorithm. *J. Mol. Graph. Model.* **38**, 314 (2012).
31. A. Jumabaev, H. Hushvaktov, A. Absanov, B. Khudaykulov, Z. Ernazarov, L. Bulavin. Vibrational spectra and computational study of amyl acetate: MEP, AIM, RDG, NCI, ELF and LOL analysis. *Ukr. J. Phys.* **69**, 742 (2024).
32. A. Jumabaev, U. Holikulov, H. Hushvaktov, A. Absanov, L. Bulavin. Interaction of valine with water molecules: Raman and DFT study. *Ukr. J. Phys.* **67**, 602 (2022).
33. U. Holikulov, A.S. Kazachenko, N. Issaoui, A.S. Kazachenko, M. Raja, O.M. Al-Dossary, Z. Xiang. The molecular structure, vibrational spectra, solvation effect, non-covalent interactions investigations of psilocin. *Spectrochim. Acta Part A: Mol. Biomol. Spectrosc.* **320**, 124600 (2024).
34. A.S. Kazachenko, N. Issaoui, U. Holikulov, O.M. Al-Dossary, I.S. Ponomarev, A.S. Kazachenko, F. Akman, L.G. Bousiakou. Noncovalent interactions in N-methylurea crystalline hydrates. *Z. Phys. Chem.* **238**, 89 (2024).
35. J.-L. Bredas. Mind the gap! *Mater. Horiz.* **1**, 17 (2014).
36. A.S. Kazachenko, U. Holikulov, N. Issaoui, O.M. Al-Dossary, I.S. Ponomarev, A.S. Kazachenko, F. Akman, L.G. Bousiakou. Theoretical and experimental approach on investigation of ethylurea-water clusters. *Z. Phys. Chem.* **238**, 683 (2024).
37. R.F.W. Bader. Definition of molecular structure: By choice or by appeal to observation? *J. Phys. Chem. A* **114**, 7431 (2010).
38. I. Rozas, I. Alkorta, J. Elguero. Behavior of ylides containing N, O, and C atoms as hydrogen bond acceptors. *Am. Chem. Soc.* **122**, 11154 (2000).
39. T.-H. Tang, E. Deretey, S.J. Knak Jensen, I.G. Csizmadia. Hydrogen bonds: Relation between lengths and electron densities at bond critical points. *Eur. Phys. J. D* **37**, 217 (2006).
40. A. Jumabaev, H. Hushvaktov, A. Absanov, I. Doroshenko, B. Khudaykulov. Experimental and computational analysis of C≡ N and C–H stretching bands in acetonitrile solutions. *Low Temp. Phys.* **51**, 202 (2025).
41. K. Arulaabaranam, G. Mani, S. Muthu. Computational assessment on wave function (ELF, LOL) analysis, molecular confirmation and molecular docking explores on 2-(5-Amino-2-Methylanilino)-4-(3-pyridyl) pyrimidine. *Chem. Data Collect.* **29**, 100525 (2020).
42. Y. Li, M. Lin, M. Tian, G. Ye, X. Zhao. DFT computational and spectroscopic studies on andrographolide from different solvent effects. *J. Mol. Liq.* **390**, 123059 (2023).
43. A. Jumabaev, B. Khudaykulov, U. Holikulov, A. Norkulov, J. Subbiah, O. Al-Dossary, H. Hushvaktov, A. Absanov, N. Issaoui. Molecular structure, vibrational spectral assignments, MEP, HOMO-LUMO, AIM, NCI, RDG, ELF, LOL properties of acetophenone and for its solutions based on DFT calculations. *Opt. Mater.* **159**, 116683 (2025).
44. B. Khudaykulov, A. Norkulov, U. Holikulov, A. Absanov, I. Doroshenko, A. Jumabaev. Raman and DFT study of non-covalent interactions in liquid benzophenone and its solutions. *Low Temp. Phys.* **51**, 220 (2025).

Received 13.05.25

А. Жумабаев, Б. Худайкулов,
С.-Дж. Коямбо-Конзапа, У. Холікулов,
Х. Хушвактов, А. Абсанов, І.Ю. Дорошенко

ДОСЛІДЖЕННЯ НЕКОВАЛЕНТНИХ ВЗАЄМОДІЙ 2-ТІОФЕНКАРБОНОВОЇ КИСЛОТИ В ЕТАНОЛІ ЗА ДОПОМОГОЮ КОЛИВАЛЬНОЇ СПЕКТРОСКОПІЇ ТА РОЗРАХУНКІВ МЕТОДОМ DFT

Спектральні смуги чистої 2-тіофенкарбонової кислоти (ТСА) та її розчину в етанолі (EtOH) досліджували в ши-

рокому діапазоні за допомогою коливальної спектроскопії (Raman та FTIR). У розчині TCA з етанолом максимуми смуг валентних C=O, O–H, і C–H коливань та смуг дихальних C–H коливань мають червоний або синій зсув. Це вказує на те, що в розчинах ймовірна наявність воднев их зв'язків, ван-дер-ваальсівської взаємодії та взаємодії гіпер-кон'югації. Аналіз методами MEPS, FMO, AIM, NCI, RDG, ELF та LOL проводився з використанням квантово-хімічного обчислювального підходу на основі теорії функціонала густини (DFT). Для візуального відображення розподілу зарядів у комплексах та визначення зарядозалежних характеристик використовувалися мапи MEPS. Граничні молекулярні орбіталі були використані для пояснення хімічної реакційної здатності TCA, його молекулярної стабільності, а також електричних і оптичних властивостей. Згідно з аналізом методами AIM, NCI та RDG, комплекси TCA та TCA-EtOH переважно мають H-зв'язки помірної міцності.

Ключові слова: вібраційна спектроскопія, розрахунок методом DFT, міжмолекулярна взаємодія, топологічні параметри.